Chemical Science

Accepted Manuscript

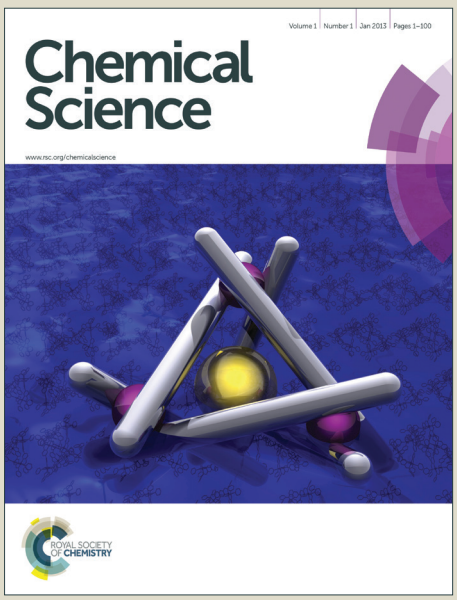

ROYAL SOCIETY OF CHEMISTRY

www.rsc.org/chemicalscience

Journal Name

RSCPublishing

ARTICLE

The kinetics of carbonyl radical ring closures.

Cite this: DOI: 10.1039/x0xx00000x

Amber N. Hancock,[a,b] and Carl H. Schiesser*[a,b]

Received 00th January 2012,
Accepted 00th January 2012

DOI: 10.1039/x0xx00000x

www.rsc.org/

Intramolecular homolytic addition reactions of acyl and oxyacyl radicals **1**, **7** – **11** have been investigated by computational techniques. Acyl radical (X = CH_2) cyclizations appear to proceed through Beckwith–Houk transition states that adopt pseudo-chair like structures, while the oxyacyl radicals (X = O) appear to behave more like sp^2-hybridized radicals in which the 6-*endo* transition states are predicted to adopt boat-like structures. G3(MP2)-RAD calculations provide activation energies (E_a) that lie in the range: 24 – 37 kJ mol^{-1} (acyl, 5-*exo*); 17 – 29 kJ mol^{-1} (oxyacyl, 5-*exo*); 32 – 41 kJ mol^{-1} (acyl, 6-*endo*); and 40 – 50 kJ mol^{-1} (oxyacyl, 6-*endo*), with associated log(A/s^{-1}) values in the expected range: 10.5 – 12.5. These data provide rate constants for 5-*exo* cyclization (k_c) of ~ 10^4 – 10^7 s^{-1} for the acyl radicals, and ~ 10^6 – 10^9 s^{-1} for the oxyacyl radicals (296K) and are in excellent agreement with the few available kinetic data. This study provides valuable new information for practitioners wishing to employ this chemistry in synthesis.

Introduction

Radical cyclization reactions have proven themselves to be among the most powerful and adaptable tools in the synthetic chemists arsenal. As a consequence of the rapid expansion of mechanistic and kinetic information that came about during the *Free Radical Renaissance Period*,[1] intramolecular radical additions and substitutions are frequently used today to generate complex polycyclic molecular frameworks through purposeful design of radical precursors and reaction conditions. The cyclization of alkyl radicals onto olefins is so well characterized that it is commonplace to exploit these reactions for advantages that include: high functional group tolerance and controlled regio/stereo-selectivity.[2] Despite the fact that this cyclization methodology has been expanded to include intramolecular additions of aryl,[3] vinyl,[4,5] and heteroatom-centred radicals,[6] relatively few examples that utilize carbonyl radicals have been reported.[7-11]

Elegant examples employing radical cyclization cascades of alkyl radicals abound and can be standard routes to the construction of interesting natural products.[12] For example, tandem radical cyclization is known to be an efficient route to bicyclo[5.4.0]undecane.[13] In contrast, synthetic strategies employing carbonyl radicals in cyclization cascades are often subject to complications because of an inability to predict accurately the rates of competing pathways. For example, Donner and co-workers recently reported the synthesis of racemic *Longianone* and analogues using acyl radical cyclization as the key synthetic step (Scheme 1).[14] The paucity of kinetic information resulted in an inability to predict that cyclization would be hindered by competing decarbonylation.

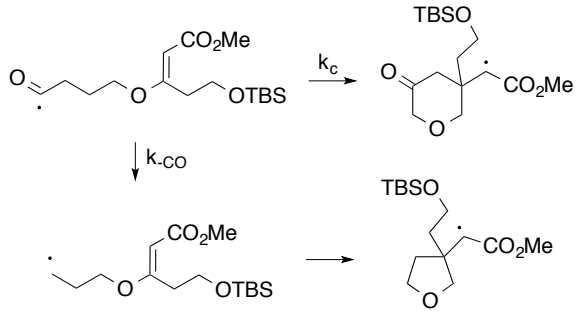

Scheme 1.

Clearly, use of carbonyl radicals in synthesis is hampered by our unfamiliarity with their relative propensities to follow competing reaction pathways. With the vast majority of free radical reactions controlled by kinetics rather than thermodynamics,[1] the availability of kinetic data for the most likely reaction pathways becomes crucial when designing syntheses based on this chemistry; the availability of kinetic data (or lack thereof) may, as a consequence, be a primary determining factor in their utility to the synthetic practitioner.

Generally, acyl radicals have enjoyed more attention in synthesis than their oxyacyl siblings because their chemistry is better understood. To exploit the full potential of the chemistry of carbonyl radicals requires a more complete understanding of

the factors governing reactivity. For radical reactions under kinetic control there exist a myriad of possible pathways that can lead to a host of products; as a consequence it is important that the subtleties of the corresponding potential energy surfaces are fully appreciated.

Of the likely decay routes for a carbonyl radical, decarboxylation/decarbonylation kinetics have been studied in the most detail. While the majority of acyl radical decarbonylations are endothermic, oxyacyl radical decarboxylations are typically exothermic indicating there may be significant reactivity differences between the two classes of radicals.[15]

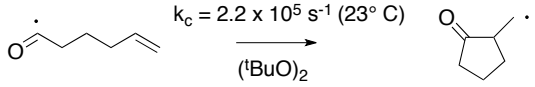

Scheme 2.

In the case of cyclization reactions of acyl radicals few rate data are available in the literature, although mechanistic studies by several groups have provided evidence for irreversible and *exo*-selective cyclization of the 5-hexenoyl radical (Scheme 2).[16-18] To date, a single directly measured intramolecular addition rate constant, at a single temperature, in a single solvent is available,[19] clearly insufficient to inform practitioners interested in methodology development using carbonyl radical addition chemistry (Scheme 2). Indirect cyclization rate data for acyl and oxyacyl radicals have been reported employing stannane mediated radical generation from acyl phenylselenides.[17,20]

Knowledge of hydrogen atom transfer kinetics can be useful for the calibration of radical cyclizations, however, for carbonyl radicals few rate constants (k_H) for hydrogen transfer are available and those that are rely on *post facto* analysis in lieu of direct measurement, which necessitates accurate knowledge of the kinetics of the competing molecular clock. For example, rate data for hydrogen transfer from tributyltin hydride have been determined using phenylselenide precursors for both acyl and oxyacyl radicals.[20,21] Unfortunately, Crich has demonstrated, that under these conditions, residual trace amounts of diphenyldiselenide react rapidly with stannanes to generate benzeneselenol,[22] a markedly more reactive hydrogen donor to carbon radicals that the stannane itself.[22-24] *Eo ipso* phenylselenides are a precarious choice of radical precursors for competition studies under stannane mediated conditions and data acquired under these conditions may not be reliable.

Experimental investigation of acyl and, even more so, oxyacyl radical reactivity is principally impeded by a paucity of suitable radical precursors for kinetic studies. Precursors for these radicals include Barton/Kim oxalates/, phenyltellurides/selenides/sulfides, aldehydes, acylhalides, carbonylphosphine oxides, acylcobalt salophen complexes and carbonylation of other radicals.[11,25,26] Unfortunately, use of these precursors often requires reaction conditions that preclude straightforward experimental kinetic analysis. To circumvent the issue of uncertainty inherent to experimental analysis of acyl and oxyacyl radical kinetics we address the lack of fundamental kinetic data through computational means.

In recent years, our group has effectively employed computational techniques to provide rate data for intramolecular reactions of radicals that are in good-to-excellent agreement with experimentally derived rate coefficients.[27-31] Taking a similar approach to the challenge at hand, herein we report kinetic parameters relevant to cyclization of systematically substituted hexenoyl and butenyloxyacyl radicals and explicate upon the origins contrasting reactivity in these carbonyl radical additions.

Computational Methods

Ab initio and DFT calculations were carried out using Gaussian 09[32] and Molpro 2009.[33] Systematic conformational searches were carried out to ensure global rather than local minima were studied. Rotational increments of 120° were employed as this resolution has been reported to adequately explore molecular conformations.[34] Geometry optimizations were performed utilizing standard gradient techniques at HF, MP2, B3LYP, and BHandHLYP levels of theory using restricted (RHF,RMP2, RB3LYP and RBHandHLYP) and unrestricted (UHF, UMP2, UB3LYP and UBHandHLYP) methods for closed and open shell systems, respectively.[35] Standard basis sets were employed in all calculations. To obtain improved energies, single point ROMP2, QCISD and CCSD(T) calculations were performed on select BHandHLYP and MP2 optimized structures. Apart from some HF calculated structures, values of $<s^2>$ never exceeded 0.81 before annihilation of the first spin contaminant. After annihilation of quartet contamination $<s^2>$ ranged from 0.75 to 0.77. Zero point energy corrections have been applied to all optimized structures and all ground and transition state structures have been verified by vibrational frequency analysis. Optimized geometries and energies for all transition structures in this study are available in the ESI.† Kinetic parameters were determined using the Eyring equation and energies obtained using the G3(MP2)-RAD method. G3(MP2)-RAD is a high-level composite method that has been shown to perform within chemical accuracy for radical reaction, hence it was selected for our study.[36]

Results and Discussion

Intramolecular additions of the 5-hexenoyl and 3-buten-1-yloxyacyl radicals (1).

Level of Theory	$\Delta E_1^{\ddagger}$	$\Delta E_2^{\ddagger}$	$\Delta E_3^{\ddagger}$	$\Delta E_4^{\ddagger}$		$\Delta E_1^{\ddagger}$	$\Delta E_2^{\ddagger}$	$\Delta E_3^{\ddagger}$	$\Delta E_4^{\ddagger}$
X = CH_2					**X = O**				
B3LYP/6-31G(d)	32.4 (30.2)[a]	75.1 (71.5)[a]	36.0 (37.2)[a]	99.6 (98.0)[a]		21.3 (19.7)[a]	92.7 (89.4)[a]	41.3 (41.0)[a]	105.5 (100.7)[a]
BHandHLYP/6-311G(d,p)	47.7 (44.5)[a]	94.4 (90.6)[a]	54.5 (54.9)[a]	121.9 (119.0)[a]		33.8 (31.6)[a]	113.6 (110.4)[a]	55.5 (54.7)[a]	146.5 (142.1)[a]
BHandHLYP/6-311++G(d,p)	47.1 (44.2)[a]	94.5 (90.5)[a]	52.6 (53.0)[a]	122.6 (119.6)[a]		33.7 (31.6)[a]	113.2 (109.9)[a]	55.3 (54.7)[a]	146.5 (142.0)[a]
BHandHLYP/cc-pVTZ	48.7 (45.7)[a]	92.8 (89.0)[a]	55.0 (55.7)[a]	120.3 (117.6)[a]		34.7 (32.4)[a]	113.0 (109.5)[a]	55.9 (55.2)[a]	145.9 (141.7)[a]
BHandHLYP/aug-cc-pVTZ	48.0 (45.1)[a]	92.3 (88.5)[a]	54.6 (55.3)[a]	120.3 (117.5)[a]		34.2 (32.0)[a]	112.4 (108.9)[a]	55.4 (54.8)[a]	145.2 (141.1)[a]
MP2/6-311++G(d,p)	74.2 (69.8)[a]	121.5 (120.6)[a]	73.5 (74.3)[a]	132.8 (132.1)[a]		58.8 (51.9)[a]	138.5 (136.6)[a]	80.6 (75.3)[a]	161.4 (158.8)[a]
ROMP2/6-311++G(d,p)[b]	44.9	93.1	44.6	103.4		33.9	112.4	52.7	132.9
QCISD/6-311++G(d,p)[b]	51.7	96.7	58.7	117.5		35.8	112.5	57.1	137.9
CCSD(T)/6-311++G(d,p)[b]	45.2	90.0	48.0	104.8		32.1	106.2	52.3	129.8
G3(MP2)-RAD[c]	36.7	80.1	44.1	100.2		23.1	99.8	41.9	123.4

[a]Values in parentheses are zero-point energy (ZPE) corrected. [b]Single point calculation optimised at BHandHLYP/6-311++G(d,p). [c] $\Delta E^{\ddagger}$ for the "forward reactions" calculated on B3LYP/6-31G(d) optimised geometry $\Delta E^{\ddagger}$=ΔE[ROCCSD(T)/6-31G(d)] – ΔE[ROMP2/6-31G(d)] + ΔE[(RO)MP2/G3MP2large] + ΔHLC + ΔSO +ΔTC[B3LYP/6-31G(d)] * 0.9989 + ΔZPVE[B3LYP/6-31G(d)] * 0.9806.

Table 1. Calculated activation energies ($\Delta E^{\ddagger}$/kJ mol^{-1}) for the intramolecular homolytic addition reactions of acyl and oxyacyl radicals 1 (Scheme 3).

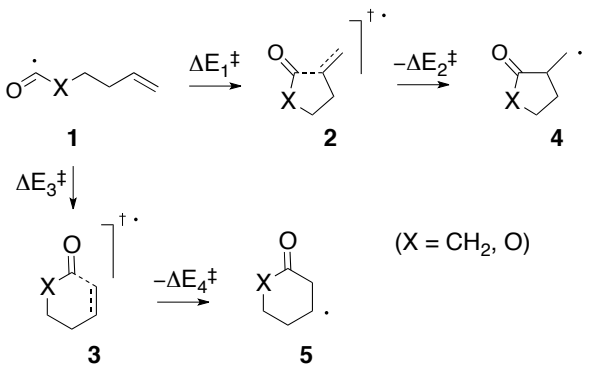

Scheme 3.

We began this study by exploring the intramolecular addition of the 5-hexenoyl and 3-buten-1-yloxyacyl radicals **1** (X = CH_2, O) (Scheme 3). These systems form the "core" of the cyclization reactions in this study, are the least computationally expensive to perform, and consequently provided an opportunity to benchmark the various computational methods employed in this study.

Extensive searching of the appropriate potential energy surface at the levels of theory employed for optimization in this work (Table S1: see ESI†) located transition states **2** and **3** for the respective 5-*exo* and 6-*endo* cyclizations of radicals **1** (Scheme 3). At all levels of theory used for optimization, the authenticity of each saddle point was verified by the presence of a single imaginary motion vector. Transition state separations of around 2.2Å are calculated for **2** and **3** (X = O), consistent with analogous alkyl radical ring closures.[35] The corresponding separations when X = CH_2 are somewhat shorter, consistent with the delocalized nature of acyl radicals,[15] that require later transition states for cyclization.

Key geometric features of these transition states calculated at the BHandHLYP/aug-cc-pVTZ level of theory are displayed in Figure 1 and are representative of those determined at other levels of theory (Figure S1: see ESI)†. Inspection of the transition structures in Figure 1 reveal that both acyl and oxyacyl radicals **1** prefer to ring-close in the 5-*exo* mode through chair-like structures, consistent with the Beckwith-Houk model for their alkyl counterparts.[37,38] Moreover, the observed preference for a chair-like transition state for the acyl

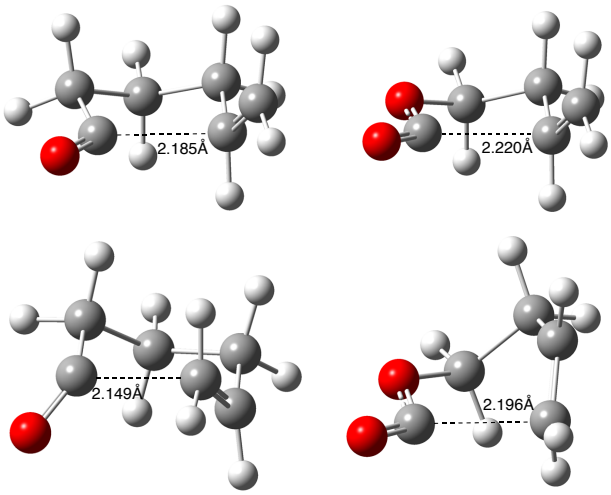

Figure 1. BHandHLYP/aug-cc-pVTZ calculated lowest energy transition states (2, 3) for the 5-*exo* (above) and 6-*endo* (below) modes of cyclization of the 5-hexenoyl (1, X = CH_2) and 3-buten-1-yloxyacyl (1, X = O) radicals.

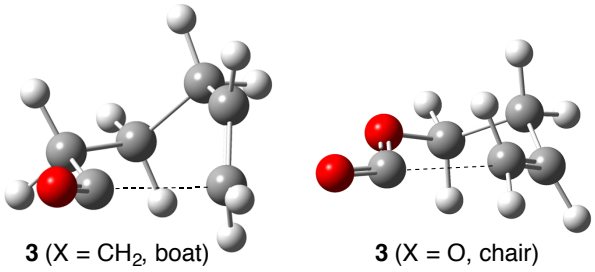

radical **1** (X = CH_2) is in accord with previous reports by Chatgilialoglu.[17]

In the 6-*endo* mode, the acyl radical transition state **3** (X = CH_2) resembles a distorted chair similar to that reported previously,[17] while at all levels of theory, **3** (X = O) prefers to adopt a distorted boat-like structure (Figure 1). Indeed this boat-like structure proved to be lower in energy than the corresponding chair (**3**, X = O, chair) by ~3 – 6 kJ mol^{-1} at non-HF levels of theory, while a similar preference for the chair-like structure (over **3**, X = CH_2, boat) was noted for the acyl radical.

Table 1 lists the energy barriers $\Delta E_1^{\ddagger} - \Delta E_4^{\ddagger}$ associated with the reaction manifold depicted in Scheme 3 calculated at key levels of theory; a full listing can be found in Table S1 in the ESI.†

All levels of theory predict that the cyclizations of **1** are exothermic, with forward barriers $\Delta E_1^{\ddagger}$ (*exo*) in the range 30 – 75 kJ mol^{-1} (acyl) and 20 – 60 kJ mol^{-1} (oxyacyl), with $\Delta E_3^{\ddagger}$ (*endo*) in the range 40 – 80 kJ mol^{-1} for both acyl and oxyacyl radicals. Reverse barriers ($\Delta E_2^{\ddagger}$, $\Delta E_4^{\ddagger}$) are calculated to be significantly larger (75 – 160 kJ mol^{-1}), depending on the level of theory. It is interesting to note that of all the methods used in this study, MP2 appears to perform the most poorly with calculated barriers that differ significantly from those calculated using other levels; even HF methods (Table S1) provide more reliable data. ROMP2, as noted previously by Radom,[39] on the other hand, provides data as reliable as the more expensive CCSD(T) method. It is also significant to note that while B3LYP/6-311G(d) provides energy barriers that are some 10 – 15 kJ mol^{-1} lower than CCSD(T)/6-311++G(d,p), they are surprisingly close to the G3(MP2)-RAD activation energies calculated at zero K.

Inspection of Table 1 also reveals that for the *exo* mode of ring closure the oxyacyl radical (**1**, X = CH_2) proceeds through a transition state **2** located some 10 – 12 kJ mol^{-1} closer to the starting radical than the corresponding acyl radical (**1**, X = O). This is consistent with **2** (X = CH_2) being a "later" transition state than its oxyacyl counterpart **2** (X = O), as discussed previously (Figure 1). Interestingly, the *endo* mode of cyclization for both radicals **1** show no such preference, with each system having a similar energy barrier (52.3 kJ mol^{-1} at CCSD(T)/6-311++G(d,p)).

Lastly, the data provided in Tables 1 and S1 provide important benchmarking information for these calculations. Clearly electron correlation is important as HF methods overestimate energy barriers. MP2 performs poorly (*vide supra*) while BHandHLYP, ROMP2, QCISD and CCSD(T) methods provide data within a few kJ mol^{-1} of each other (with the same basis set), and certainly within the accuracy required for this study. The data also show that within the triple-ζ basis sets used, Pople and Dunning sets perform as well as each other, and that diffuse functions appear not to play a major role for the systems in this study.

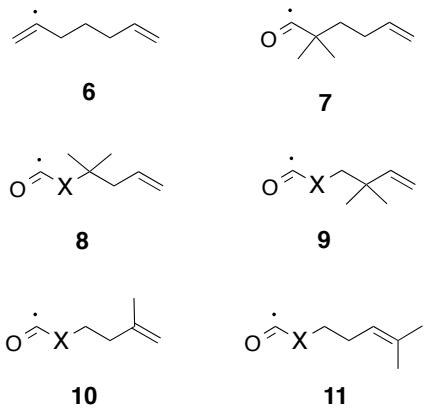

Radical	k_c / s^{-1} exo	k_c / s^{-1} endo	log(A/s^{-1}) exo	log(A/s^{-1}) endo	E_a / kJ mol^{-1} exo	E_a / kJ mol^{-1} endo
X = CH_2						
1	1.04 x 10^5	9.55 x 10^3	11.5	11.0	36.7	40.2
7	1.79 x 10^7	1.60 x 10^5	11.6	10.9	24.6	32.8
8	4.32 x 10^6	2.36 x 10^5	11.9	11.4	29.8	34.5
9	2.50 x 10^5	1.01 x 10^4	11.6	11.2	35.1	41.2
10	3.28 x 10^4	2.06 x 10^5	11.3	11.2	38.4	33.6
11	1.15 x 10^6	1.21 x 10^5	11.9	10.7	32.9	35.9
X = O						
1	1.57 x 10^7	3.74 x 10^3	11.7	11.4	25.5	44.3
8	6.98 x 10^8	7.97 x 10^2	11.9	11.7	17.3	49.8
9	5.16 x 10^7	3.10 x 10^4	11.9	11.7	23.7	40.8
10	4.62 x 10^6	3.37 x 10^4	11.7	11.7	28.5	40.6
11	6.74 x 10^8	2.98 x 10^2	12.4	11.1	25.1	48.7

Table 2. G3(MP2)-RAD calculated Arrhenius parameters (E_a, logA) and rate constants (k_c) for ring-closure of 1 and substituted acyl and oxyacyl radicals 7 – 11 at 296K.

Determination of kinetic parameters.

We next turned our attention to determining important kinetic parameters for these cyclization reactions (Scheme 3). As mentioned above, the G3(MP2)-RAD method was selected for this purpose as this method has been shown to afford rate data for several intramolecular radical reactions within chemical accuracy; this methodology has been described previously.[27–31]

When applied to radicals **1**, G3(MP2)-RAD provided gas-phase rate constants (k_c) of 1.0 x 10^5 and 1.6 x 10^7 s^{-1} at 296K for the *exo* modes of cyclization of the acyl and oxyacyl radicals (**1**) respectively. The former is in excellent agreement with the experimentally determined value of 2.2 x 10^5 s^{-1} determined at 296K in di-*tert*-butyl peroxide by Ingold and coworkers using laser flash techniques.[19] This outcome provides confidence in our computational approach for these

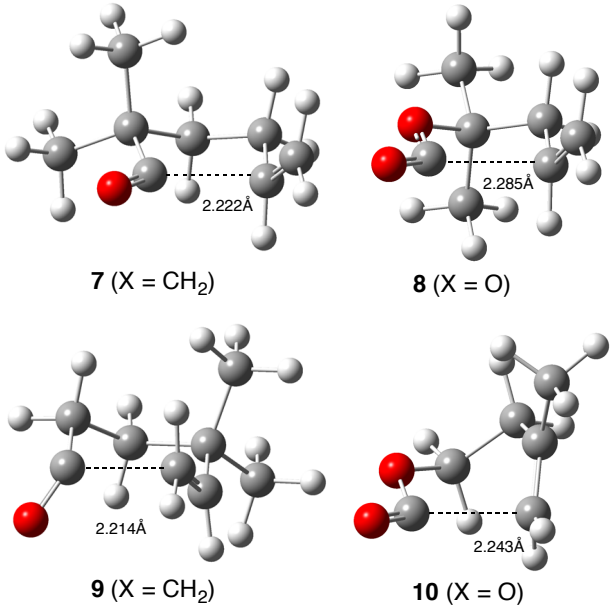

Figure 2. Selected B3LYP/6-31G(d) calculated lowest energy transition states for the cyclization of radicals 7 – 10.

radicals.

As mentioned previously, there are no reliable experimental kinetic data for the cyclization of the oxyacyl radical (**1**, X = O). Despite this, it is useful to compare our computational data with those reported by Newcomb and coworkers.[20] At the time, no kinetic experiments had been performed on oxyacyl radicals such as **1**. Using the best cyclization data available,[40] together with freshly determined data for k_H,[20] Newcomb was able to estimate k_c for **1** to be 4 x 10^6 s^{-1} at 353K, well over an order of magnitude slower than that determined in this study (8 x 10^7 s^{-1}) when adjusted to 353K. The authors were very aware that the product ratio data reported by Bachi[40] may have been affected by impure phenylselenide precursors and conclude by stating "one must be aware of the fact that generation of PhSeH from small impurities of PhSeSePh or from photolyis of the precursor can be problematical".[20]

We are confident that our calculated value for k_c of 8 x 10^7 s^{-1} (corrected to 353K) for the 5-*exo* mode of cyclization of **1** is approximately correct. This, together with the knowledge that PhSeH delivers hydrogen atom to primary alkyl radicals with a rate constant (k_H) of 4 x 10^9 s^{-1} at 353K,[23] and assuming that a similar value of k_H operates for oyacyl radicals, it is easy to show that a virtually undetectable 0.25% PhSeSePh impurity in Bachi's phenylselenide precursor for **1** will have significantly distorted the value of k_c (calculated from the experimentally determined product ratio) from our value to that reported by Newcomb (4 x 10^6 s^{-1}). This, in itself, is further validation of the computational approach that we have adopted for determining rate data for problematic systems such as those in question. Indeed, for all of the reasons discussed above, the calculated rate data that result from this study provide greater certainty than the experimental estimates reported previously that can be distorted by over an order of magnitude.

It is well established that acyl radicals are stabilised by resonance, while oxyacyl radicals are less so and, as a consequence, oxyacyl radicals resemble more closely sp^2 hybridised radicals in both structure and reactivity.[11,15] This is evident in their measured and calculated infrared carbonyl stretching frequencies. For example, the acetyl radical absorbs at 1864 cm^{-1}, some 90 cm^{-1} higher than the methoxyacyl radical.[15,41] It is probably more instructive, therefore, to compare the calculated rate constant for **1** (X = O) with that of the corresponding vinyl radical **6** which is reported to ring close with a value of k_c of 2 x 10^7 s^{-1} at 296K.[42] This value closely resembles that calculated for **1** (X = O) (1.6 x 10^7 s^{-1}) confirming that the oxyacyl radical, like **6** cyclizes with a typical rate constant of an sp^2-hybridized radical, whereas the analogous acyl radical reacts more slowly.

Confident in our ability to determine reliable rate data for acyl and oxyacyl radicals, we set about determining Arrhenius parameters for **1** and substituted analogues (**7** – **11**). Selected B3LYP/6-31G(d) transition state structures for the *exo* and *endo* modes of cyclization of radicals **7** – **10** are provided in Figure 2, with the remaining structures available in the ESI (Figure S2), together with those for **1**.† It is interesting to note that like their unsubstituted counterparts, radicals **7** – **11** are predicted to ring-close in the 5-*exo* mode through chair-like transitions states, and in the 6-*endo* mode through distorted chair-like structures for the acyl radicals, and through distorted boat-like structures for the oxyacyl radicals.

When the B3LYP data are introduced into the G3(MP2)-RAD method as described previously,[31] the Arrhenius parameters and rate data listed in Table 2 are obtained. For the 5-*exo* mode of ring closure, values of k_c are in the range ~10^4 – 10^7 s^{-1} for the acyl radicals, and ~10^6 – 10^8 s^{-1} for the oxyacyl radicals at 296K. As expected, radicals **7** – **9** benefit from *Thorpe-Ingold* rate enhancement[43] that manifests itself in lower activation energies (E_a) for 5-*exo* cyclization and in "earlier" transition states (Figure S2). For example, B3LYP/6-31G(d) 5-*exo* transition state separations of 2.221 – 2.234Å are calculated for **7** – **9** (X = CH_2) using B3LYP/6-31G(d), significantly longer (18 – 25%) than the parent **1** (2.178Å); a similar trend is observed in the oxyacyl series (26 – 30%). In addition, *gem*-dimethyl substitution in radicals **7** – **9** lowers E_a by some 2 – 12 kJ mol^{-1} over the parent **1** for both acyl and oxyacyl radicals. G3(MP2)-RAD calculations predict that the 2,2-dimethyl-5-hexenoyl radical (**7**, X = CH_2) cyclizes with a 5-*exo* rate constant (k_c) of 1.8 x 10^7 s^{-1} at 296K, the fastest in the acyl radical series and some two orders of magnitude faster than the parent **1**. On the other hand, the analogous reaction involving the 5-methyl-5-hexenoyl radical (**10**, X = CH_2) is predicted to be the slowest 5-*exo* cyclization in the series, with a value for k_c of only 3.3 x 10^4 s^{-1} at the same temperature. Similar trends are observed for substituted 3-buten-1-yloxyacyl (**8** – **10**, Table 2) and 5-hexenyl radicals, with the 2,2-dimethyl-5-hexenyl (3.6 x 10^6 s^{-1}, 298K) and 5-methyl-5-hexenyl (5.3 x 10^3 s^{-1}, 298K) radicals being significantly faster and slower than the parent 5-hexenyl radical (2.3 x 10^5 s^{-1}, 298K) respectively.[37]

It is not unexpected that radicals **10** react more slowly than their siblings, this result is a consequence of the presence of a substituent on the proximal end of the olefin, and is in accord with the *Guidelines for Radical Reactions*.[2,44] 5-*Exo* cyclizations of radicals **11** are assisted by stabilization of the transition state through hyperconjugation into the methyl substituents at the developing radical centre at the distal end of the olefin.

For the 6-*endo* mode of cyclization, the trends are less obvious. In the case of the acyl radical (X = CH_2), the predicted values of k_c qualitatively mirror the trend observed for the 5-hexenyl radical, which is not surprising given that both systems cyclize through distorted chair-like transition states.[37]

For the oxyacyl system (X = O), the comparisons are less clear because of the preferred chair-like transition state for ring-closure. What is evident is that these radicals are more sensitive to ring strain and substitution resulting in a greater disposition toward 5-*exo* cyclization than their acyl counterparts. We attribute this observation to the increased sp^2 character of these radicals. Similar, but more limited, observations have been reported for some vinyl radical and aryl radicals.[37,40,45]

Conclusions

The computational work described in this paper predict that acyl radicals **1**, **7** – **11** (X = CH_2) prefer to cyclize through Beckwith–Houk transition states that adopt pseudo-chair like structures, while the oxyacyl radicals (X = O) appear to behave more like sp^2-hybridized radicals in which the 6-*endo* transition states are predicted to adopt boat-like structures. In the 5-*exo* mode of cyclization, rate constants (k_c) of ~ 10^4 – 10^7 s^{-1} are calculated using G3(MP2)-RAD for the acyl radicals, and ~ 10^6 – 10^9 s^{-1} for the oxyacyl radicals (296K). These rate constants are affected by substitution and, as expected, derive benefit through *Thorpe-Ingold* rate enhancement. While there is a clear preference for 5-*exo* cyclization for the majority of the radicals studied, most notably **10** (X = CH_2) is predicted to cyclize preferably in the 6-*endo* mode, in accordance with the *Guidelines for Radical Reactions*. These data provide important information for practitioners wishing to employ these radicals in synthesis.

Acknowledgements

Generous support of the Australian Research Council through the Centres of Excellence Scheme is gratefully acknowledged. Allocations of computing resources by the National Computing Infrastructure (NCI) National Facility and the Victorian Life Science Computation Initiative (VLSCI) are also gratefully acknowledged.

Notes and references

[a]ARC Centre of Excellence for Free Radical Chemistry and Biotechnology, Australia
[b] School of Chemistry and Bio21 Molecular Science and Biotechnology Institute, The University of Melbourne, Victoria, 3010, Australia.

Email: carlhs@unimelb.edu.au; Fax: +61 3 9347 8189; Tel: +61 3 8344 2432

* Corresponding author

† Electronic Supplementary Information (ESI) available: Table S1, Figures S1 – S3, Gaussian Archive Entries of all transition states calculated in this work. 49 Pages. See DOI: 10.1039/b000000x/

1. A. L. J. Beckwith and C. H. Schiesser, *Org. Biomol. Chem*., 2011, **19**, 1736–1743.
2. A. N. Hancock and C. H. Schiesser, *Chem. Commun*., 2013, **49**, 9892–9895.
3. L. E. Peisino and A. B. Pierini, *J. Org. Chem*., 2013, **78**, 4719–4729. K. C. Majumdar, N. Kundu, *J. Heterocycl. Chem*, 2008, **45**, 2008, 1039–1044. W. Wang , J.-T. Lu , H.-L. Zhang, Z.-F. Shi, J. Wen , X.-P. Cao, *J. Org. Chem*., 2014, **79**, 122-127.
4. H. Yokoe, C. Mitsuhashi, Y. Matsuoka, T. Yoshimura, M. Yoshida and K. Shishido, *J. Am. Chem. Soc*., 2011, **133**, 8854–8857.
5. G. Stork, F. West, H. Y. Lee, R. Isaacs, S. Manabe *J. Am. Chem. Soc*. 1996, **118**, 10660–10661. G. Stork, *Med. Res. Rev*., 1999, **19**, 370–387.
6. J. Hartung, T. Gottwald, K. Spehar, *Synthesis* 2002, **11**, 1469–1498. A. C. Callier-Dublanchet, J. Cassayre, F. Gagosz, B. Quiclet-Sire, L. A. Sharp, S. Z. Zard, *Tetrahedron* 2008, **64**, 4803–4816.
7. C. D. Donner and M. I. Casana, *Tetrahedron Lett*., 2012, **53**, 1105–1107.
8. J. E. Forbes, R. N. Saicic and S. Z. Zard, *Tetrahedron*, 1999, **55**, 3791–3802.
9. G. A. Kraus and F. Liu, *Tetrahedron Lett*., 2012, **53**, 111–114.
10. K.-i. Yamada, T. Sato, M. Hosoi, Y. Yamamoto and K. Tomioka, *Chem. Pharm. Bull*., 2010, **58**, 1511–1516.
11. C. Chatgilaloglu, D. Crich, M. Komatsu and I. Ryu, *Chem. Rev*. 1999, **99**, 1991–2069.
12. Giese, B. Kopping, T. Gobel, J. Dickhaut, G. Thoma, K. J. Kulicke and O. R. F. Trach, *Radical Cyclization Reactions*, Wiley and Sons, New York, vol. 48, 1996, pp 301–340.
13. S. W. Grant, K. D. Zhu, Y. Zhang and S. L. Castle, *Org. Lett*., 2006, **8**, 1867–1869.
14. H. M. Aitken, C. H. Schiesser and C. D. Donner, *Aust. J. Chem*., 2011, **64**, 409–415.
15. T. Morihovitis, C. H. Schiesser and M. A. Skidmore, *Perkin 2*, 1999, 2041–2047.
16. D. L. Boger and R. J. Mathvink, *J. Org. Chem*., 1992, **57**, 1429–1443.
17. C. Chatgilialoglu, C. Ferreri, M. Lucarini, A. Venturini and A. A. Zavitsas, *Chem. - Eur. J*., 1997, **3**, 376–386.
18. D. Crich and D. Batty, *Perkin 1*, 1992, 3193–3204.
19. C. E. Brown, A. G. Neville, D. M. Rayner, K. U. Ingold and J. Lusztyk, *Aust. J. Chem*., 1995, **48**, 363–379.
20. P. A. Simakov, F. N. Martinez, J. H. Horner and M. Newcomb, *J. Org. Chem*., 1998, **63**, 1226–1232.
21. C. Chatgilialoglu, C. Ferreri, M. Lucarini, P. Pedrielli and G. F. Pedulli, *Organometallics*, 1995, **14**, 2672–2676.
22. D. Crich and Q. W. Yao, *J. Org. Chem.*, 1995, **60**, 84–88.
23. M. Newcomb, *Tetrahedron*, 1993, **49**, 1151–1176.
24. D. Crich, X.-Y. Jiaao, Q. Yao and J. S. Harwood, *J. Org. Chem*., 1996, **61**, 2368–2373.
25 M. A. Lucas and C. H. Schiesser, *J. Org. Chem.*, 1996, **61**, 5754–5761.
26. M. A. Lucas and C. H. Schiesser, *J. Org. Chem.*, 1998, **63**, 3032–3036.
27. H. M. Aitken, A. N. Hancock and C. H. Schiesser, *Chem. Commun*., 2012, 48, 8326–8328.
28. S. H. Kyne, C.-Y. Lin, I. Ryu, M. L. Coote and C. H. Schiesser, *Chem. Commun*., 2010, **46**, 6521–6523.
29. H. M. Aitken, S. M. Horvat, C. H. Schiesser, C.-Y. Lin and M. L. Coote, *Int. J. Chem. Kinet*., 2011, **43**, 51-59.
30. H. M. Aitken, S. M. Horvat, M. L. Coote, C.-Y. Lin and C. H. Schiesser, *Aust. J. Chem*., 2013, **66**, 323–329.
31. S. Lobachevsky, C. H. Schiesser, C.-Y. Lin and M. L. Coote, *J. Phys. Chem. A*, 2008, **112**, 13622–13627.
32. M. J. Frisch, G. W. Trucks, H. B. Schlegel, G. E. Scuseria, M. A. Robb, J. R. Cheeseman, G. Scalmani, V. Barone, B. Mennucci, G. A. Petersson, H. Nakatsujo, M. Caricato, X. Li, H. P. Hratchian, A. F.

Izmaylov, J. Bloino, G. Zheng, J. L. Sonngnberg, M. Hada, M. Ehara, K. Toyota, R. Fukuda, J. Hasegawa, M. Ishida, T. Nakajima, Y. Honda, O. Kitao, H. Nakai, T. Vreven, J. A. M. Jr., J. E. Peralta, F. Ogliaro, M. Bearpark, J. J. Heyd, E. Brothers, K. N. Kudin, V. N. Staroverov, R. Kobayashi, J. Normand, K. Raghavarachari, A. Rendell, J. C. Burant, S. S. Iyengar, J. Tomasi, M. Cossi, N. Rega, J. M. Millam, M. Klene, J. E. Knox, J. B. Cross, V. Bakken, C. Adami, J. Jaramilli, R. Gomperts, R. E. Stratmann, O. Yazyev, A. J. Austin, R. Cammi, C. Pomelli, J. W. Ochterski, R. L. Martin, K. Morokuma, V. G. Zahrzewski, G. A. Voth, P. Salvador, J. J. Dannenberg, S. Dapprich, A. D. Daniels, O. Farkas, J. B. Farkas, J. B. Foresman, J. V. Ortiz, J. Cioslowski and D. J. Fox, Gaussian 09, Gaussian Inc., Wallingford CT, Revision C. 1.

33. H. J. Werner, P. J. Knowles, R. Lindh, F. R. Manby, M. Schutz, P. Celani, T. Korona, G. Rauhut, R. D. Amos, A. Bernhardsson, A. Berning, D. L. Cooper, M. J. O. Deegan, A. J. Dobbyn, F. Eckert, C. Hampet, G. Hetzer, A. W. Lloyd, S. J. McNicholas, W. Meyer, M. E. Mura, A. Nicklass, P. Palmieri, R. Pitzer, U. Schumman, H. Stoll, A. J. Stone, R. Tarroni and T. Thorsteinsson, MOLPRO: A Package of ab initio programs, University College Cardiff Consultants Limited, Cardiff, Revision 2009:1 edn., 2009.
34. E. I. Izgorodina, C.-Y. Lin and M. L. Coote, *PhysChemChemPhys*., 2007, **9**, 2507–2516.
35. W. J. Hehre, L. Radom, P. v. R. Schleyer and J. A. Pople, *Ab Initio Molecular Orbital Theory*, Wiley, New York, 1986.
36. D. J. Henry, M. B. Sullivan and L. Radom, *J. Chem. Phys*., 2003, **118**, 4849–4860.
37. A. L. J. Beckwith, C. H. Schiesser, *Tetrahedron*, 1985, **41**, 3925–3941.
38. D. C. Spellmeyer and K. N. Houk, *J. Org. Chem.*, 1987, **52**, 959–974.
39. C. J. Parkinson, P. M. Mayer and L. Radom, *Perkin 2*, 1999, 2305–2313.
40. M. D. Bachi and E. Bosch, *J. Org. Chem.*, 1992, **57**, 4696–4705.
41. C. E. Brown, A. G. Neville, D. M. Rayner, K. U. Ingold and J. Lusztyk, *Aust. J. Chem.*, 1995, **48**, 363–379.
42. A. L. J. Beckwith and D.M. O'Shea, *Tetrahedron Lett*., 1986, **27**, 4525–4528.
43. R. M. Beesley, C. K. Ingold, J. F. Thorpe, *J. Chem. Soc*., *Trans*., 1915, **107**, 1080–1106.
44. A. L. J. Beckwith, C. J. Easton and A.K. Serelis, *J. Chem. Soc. Chem. Commun*., 1980, 482–483.
45. A. L. J. Beckwith, W. B. Gara, *J. Chem. Soc., Perkin Trans. 2*, 1975, **6**, 593–600.